Scientia Iranica A (2015) 22(1), 144–156

Sharif University of Technology
Scientia Iranica
Transactions A: Civil Engineering
www.scientiairanica.com

Research Note

Numerical study on flexural strengthening of squat RC shear wall using FRP laminates

F. Shadan[a,*], A. Khaloo[a] and P. Shadan[b]

a. *Department of Civil Engineering, Sharif University of Technology, Tehran, Iran.*
b. *Department of Civil and Environmental Engineering, Amirkabir University of Technology, Tehran, Iran.*

Received 14 February 2012; received in revised form 12 March 2014; accepted 22 November 2014

KEYWORDS
Shear wall;
Fibre reinforced polymer;
Strengthening;
Reinforcement details;
Anchorage system.

Abstract. Shear wall has been widely used in RC structures due to its high initial stiffness and lateral load capacity. Hence, the behavior and effectiveness of retrofitting technique on shear wall are needed to be investigated widely. In this paper, a numerical analysis was performed using LS-DYNA finite element program to predict the behavior of squat RC shear wall strengthened by fiber reinforced polymer in flexure. The strengthening scheme was conducted by externally bonding vertical layers of FRP on each side of the wall and anchoring them at the wall base with a structural steel angle bolted to the support. Numerical results were validated against experimental data. Then, the influences of number of FRP layers, anchorage system, percentage of horizontal web reinforcement, percentage of vertical web reinforcement and percentage of vertical reinforcement in the boundary element were investigated. The results showed that the scheme can significantly improve the behavior of the RC shear wall. In addition, the behavior of strengthened wall and strengthening scheme strongly depend on the amount of web reinforcement which can also change the failure mode.

1. Introduction

Based on high initial stiffness and lateral load capacity of shear wall, its usage as a common type of lateral load resisting system in RC structures has been increased. Old buildings shear wall which has been designed based on older building codes, in new codes sight do not have enough stiffness, ductility and strength. Thus major earthquakes subjected them to severe damages. Hence, the behavior and effectiveness of retrofitting technique on shear wall are needed to be investigated widely. Among several available techniques for retrofitting RC structures, Fiber Reinforced Polymer (FRP) is quite effective due to its high strength-weight ratio, high resistance to corrosion, and easy handling and installation [1]. Several researchers have investigated the behavior of RC members retrofitted with FRP like beams and columns since 1990 [2-6]. However, application of FRP laminates on RC walls has attracted less attention from researchers.

Lombard performed strengthening of shear walls using carbon fiber reinforced polymers externally bonded to the two faces of the wall [7]. Uni-directional carbon fibers aligned in the vertical and horizontal direction were used to increase the strength and stiffness of the wall. Other rehabilitation schemes also have been investigated experimentally and showed that use of FRP in rehabilitation of wall is promising [8-10]. These available experimental studies on retrofitting of RC shear walls focused on the effectiveness of the

*. *Corresponding author. Tel.: +98 21 66164211; Fax: +98 21 66014828*
E-mail addresses: f_shadan@alum.sharif.edu (F. Shadan); khaloo@sharif.edu (A. Khaloo); p_shadan@aut.ac.ir (P. Shadan)

technique rather than attempting to quantify effects of different parameters. For instance, the structural behavior of RC shear walls strongly depends on aspect ratio and reinforcement details which can change failure mode and flexural capacity of the wall. Furthermore, failure mode has considerable influence on the effectiveness of strengthening technique with FRP.

In this study, predictions were acquired using LS-DYNA [11] finite element program widely used for nonlinear analysis of structures. The adequacy of the numerical approach is verified by comparison between numerical results and experimental data tested by Lombard et al. [7]. Then, a numerical investigation was performed to predict the behavior of RC squat shear wall strengthened by fiber reinforced polymer. Influence of a number of FRP layers, anchorage system, various percentages of horizontal and vertical web reinforcement and vertical reinforcement on boundary elements of the wall were investigated. In addition, effect of these parameters on the hysteretic response characteristics of the strengthened wall, such as strength, ductility, dissipated energy and stiffness degradation, was studied.

2. Finite-element modeling

The validity of finite element modelling has been verified by testing against experimental data conducted by Lombard et al. [7]. Primarily, a brief description of experimental setup data reported in [7] and utilized as base information for further parametric studies is prepared.

Two of four reinforced concrete shear wall specimens were selected for numerical verification. Each specimen had a rectangular cross section of 100 mm thick, 1500 mm wide and a height of 1795 mm. In addition, they had an aspect ratio of 1.2 classified as squat shear wall [12], and were designed to have sufficient shear strength, and failed in a ductile flexural manner [7]. The walls were constructed using 40 MPa concrete and 10 mm deformed steel bars (f_y = 412 MPa). Details of the test specimen are shown in Figure 1.

One of the selected experimental specimens for checking numerical approach was tested in its original state as a control wall, whereas the other selected specimen was strengthened with applying uni-directional carbon fiber laminates aligned in vertical and horizontal direction to the undamaged as-built wall. The carbon fiber laminates had a tensile strength of 3480 MPa, a tensile modulus of 230 GPa and a thickness of 0.11 mm. The strengthened wall had one horizontal and two vertical layers of FRP externally bonded on each face of the wall. Moreover, the vertical layers of FRP were anchored at the wall base with a structural steel angle bolted to the support. Figure 2 shows the way of applying carbon fiber laminates and anchoring system on strengthened wall. A hydraulic actuator supported by a reaction frame applied the lateral load at the top of the specimen through a horizontal cap beam. Subsequently, the specimens were tested in the in-plane direction in reverse cyclic loading, which is according to a predetermined quasi-static loading sequence.

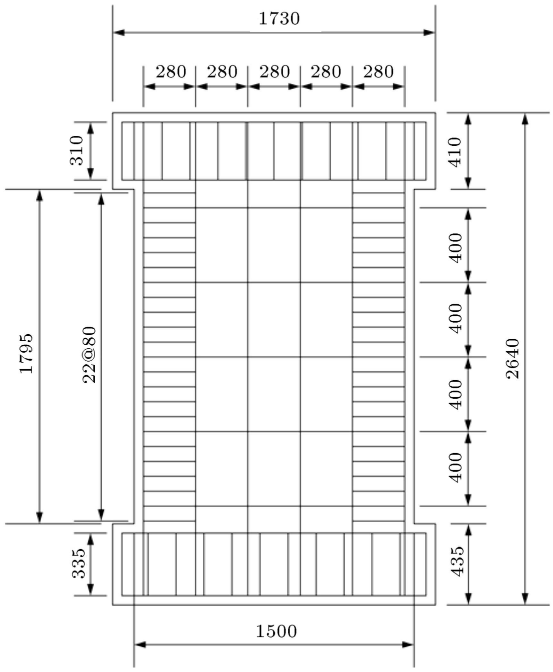

Figure 1. Geometry and reinforcement details for reinforced concrete shear wall specimen [7] (units in mm).

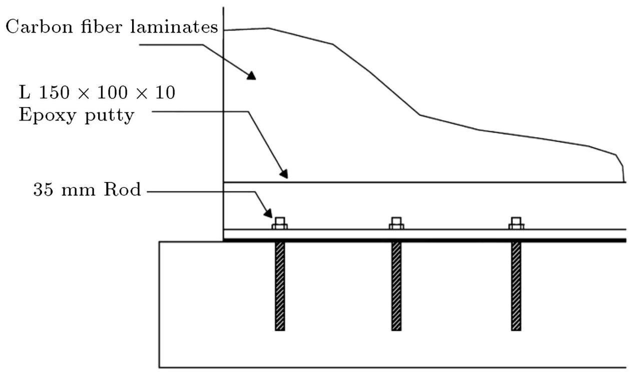

Figure 2. CFRP laminates and anchorage system position on strengthened wall [7] (units in mm).

To simulate specimens precisely, almost all details of them were considered. For this purpose, in addition to the concrete wall, the reinforcements and the FRP laminates, the slab beam, the top beam, the angles and the bolts were modeled too. The concrete wall was modeled with eight node solid elements. The reinforced bars and bolts were simulated with two node truss elements. Four node shell elements were used to model the FRP laminates and the steel angles

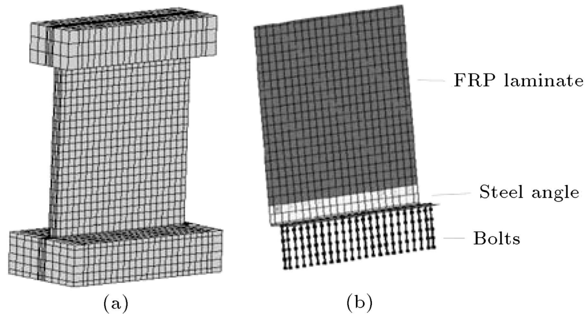

Figure 3. FE meshes: (a) Concrete wall; and (b) strengthening system.

(Figure 3). Based on the results obtained from other researchers [13], it was decided to use same node at the intersection of the concrete and reinforcements mesh. As a result, they are not able to slip and form a perfect compatibility of strains between concrete and steel. Similarly, studies done by some researchers [14,15] suggest that the nodes link concrete and FRP mesh can be shared. Therefore, a perfect bond was assumed between them too.

The boundary condition contains fixed end to the base of the slab beam, and lateral load to the center of the top beam, as the experimental setup which was modeled by considering zero displacement at the bottom surface nods, and nonzero displacement according to predetermined loading.

3. Material constitutive behaviour

Each material data in LS-DYNA program is represented by a number. The program contains several materials models that can be used to represent materials such as concrete, steel and FRP. Material type 84 (MAT_WINFRITH_CONCRETE model), material type 3 (MAT_PLASTIC_KINMATIC model) and material type 22 (MAT_COMPOSITE_DAMAGE model) were used for modelling the concrete, the steel and the FRP, respectively [11]. Hence, their input material properties and models are just briefly discussed. The values used in the input file corresponded to the experimental data.

3.1. Concrete

The WINFRITH concrete model is a basic plasticity model that contains the third stress invariant for treating both triaxial compression and triaxial extension, like Mohr-Coulomb behavior. The plasticity part of this model is based on the shear failure surface proposed by Ottosen [16]. This model also includes strain softening in tension with an attempt to regularization via crack opening width, fracture energy and aggregate size. Concrete cracks in tension with up to three orthogonal crack planes per elements. The WINFRITH concrete model is a smeared crack model which through adjusting the stiffness matrix, the effect of crack is considered as described in [11]. In this approach, based on the inputted crack width and aggregate size, this model assumes that the shear can be transferred across the crack. Furthermore, the stress decays as a function of crack width after initiation of tensile crack. This model was developed by Broadhouse and Neilson [17] and Broadhouse [18] over many years and has been validated against experiments [11]. The parameters required by this formulation are as follows.

The uniaxial compressive and tensile strength of the concrete f'_c and f'_t which corresponded to the experimental data were:

$$f'_c = 40 \text{ MPa}, \tag{1}$$

$$f'_t = 3.4 \text{ MPa}. \tag{2}$$

The initial tangent modulus of elasticity of the concrete E_c taken as the value suggested by ACI committee 318 [19] is:

$$E_c = 4700\sqrt{f'_c}. \tag{3}$$

The Poisson's ratio of the concrete v_c was assumed to be:

$$v_c = 0.2. \tag{4}$$

The aggregate size, i.e. max aggregate diameter, is supposed to be 32 mm. The effects of strain rate were not included and the crack width w, at which crack-normal tensile stress goes to zero [11], was taken as:

$$w = 0.05\ mm. \tag{5}$$

3.2. Steel

The steel bars and steel parts of the specimens were modeled as elastic perfectly plastic material by using the PLASTIC KINEMATIC model, which is provided for modeling isotropic and kinematic hardening plasticity as described in [11]. In this approach, the material behaves elastically up to yield stress. Since steel yields, the stress remains at the yield level. The required parameter for this model are yield stress, young's modulus and Poisson's ratio. The yield stress of the steel σ_y used in the specimens was assumed to be:

$$\sigma_y = 412 \text{ MPa}. \tag{6}$$

The Poisson's ratio of the steel v_s was selected as 0.3 and the young's modulus of the steel E_s used in analysis is:

$$E_s = 200 \text{ GPa}. \tag{7}$$

3.3. FRP

The Composite Damage model was presented for modeling orthotropic material with brittle failure as

Table 1. Material properties of CFRP used in the analysis.

Elastic modulus (GPa)	Poisson's ratio	Shear modulus (GPa)	Shear strength (MPa)	Longitudinal tensile strength (MPa)	Transverse tensile strength (MPa)	Transverse compressive strength (MPa)	Thickness (mm)
$E_1 = 230$	$v_{21} = 0.17$	$G_{12} = 3.27$					
$E_2 = 3.034$	$v_{31} = 0.17$	$G_{23} = 1.86$	700	3480	740	740	0.11
$E_3 = 3.034$	$v_{32} = 0.3$	$G_{31} = 3.27$					

described in [11]. In this study, failure criteria follow the criteria defined by Chang-Chang model [20,21]. In this approach, three failure criteria are considered through using five material parameters: longitudinal tensile strength, S_1, transverse tensile strength, S_2, shear strength, S_{12}, transverse compressive strength, C_2, and nonlinear shear stress parameter, α.

The shearing term of a fiber matrix, which is the ratio of the shear stress to the shear strength expands each damage mode, is:

$$\bar{\tau} = \frac{\frac{\tau_{12}^2}{2G_{12}} + \frac{3}{4}\alpha\tau_{12}^4}{\frac{s_{12}^2}{2G_{12}} + \frac{3}{4}\alpha s_{12}^4}. \tag{8}$$

The matrix cracking failure criteria, the first mode, has the following form:

$$F_{\text{matrix}} = \left(\frac{\sigma_2}{s_2}\right)^2 + \bar{\tau}, \tag{9}$$

when $F_{\text{matrix}} > 1$, it is assumed that the failure is occurred and the material constants of E_2, G_{12}, v_1 and v_2 are set to zero.

The compression failure is the second mode with the failure criteria determined from:

$$F_{\text{comp}} = \left(\frac{\sigma_2}{2s_{12}}\right)^2 + \left[\left(\frac{c_2}{2s_{12}}\right)^2 - 1\right]\frac{\sigma_2}{c_2} + \bar{\tau}, \tag{10}$$

when $F_{\text{comp}} > 1$, it is assumed that the failure is occurred and the material constants of E_2, v_1 and v_2 are set to zero.

The final mode of failure is caused by fiber breakage:

$$F_{\text{fiber}} = \left(\frac{\sigma_1}{s_1}\right)^2 + \bar{\tau}. \tag{11}$$

In this study, the flexural strengthening was done by adding CFRP laminates due to its high tensile strength and modulus. The material properties of CFRP used in the analysis are shown in Table 1.

The fiber orientation of uni-directional CFRP laminate was determined by material axis option in LS-DYNA program. It is worth noting that FRP has the highest stiffness and strength in its fiber direction which should be indicated in analysis correctly.

4. Verification of the proposed models

The results of the FE modelling and the experimental data for load versus horizontal deflection of the control wall and the strengthened wall are compared in Figure 4. A good agreement is observed between the numerical results and the experimental data.

Hence, the proposed FE model is proved to be able to simulate the behaviour of strengthened RC shear wall with FRP laminates properly.

5. Numerical analysis

In the numerical analysis, the strengthened wall, which is validated against experimental data, was considered. Then, influence of some parameters such as number

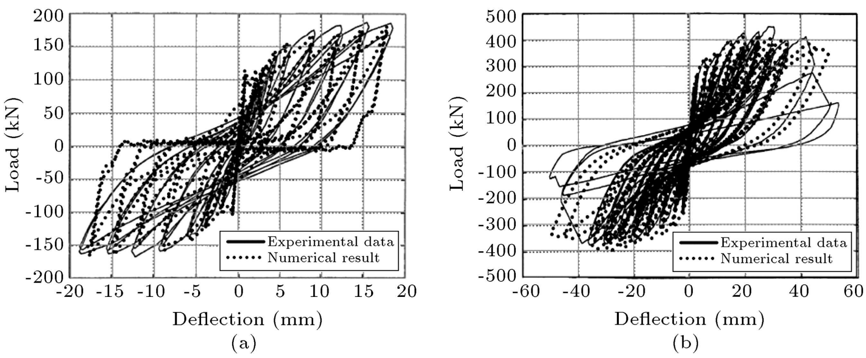

Figure 4. Comparison of numerical and experimental results: (a) Control wall; and (b) strengthened wall.

of FRP layers, anchorage system, web reinforcement ratio and various percentages of vertical reinforcement in the boundary elements on strengthening with the FRP laminates and behavior of the strengthened RC shear wall was investigated under reversed cyclic load.

5.1. Number of FRP layers

With the purpose of presenting a base for comparison, an ordinary reinforced concrete wall without strengthening as Control Wall (CW) was considered. However, other strengthened specimen with increasing number of vertical CFRP layers up to 4 was provided in order to show how FRP changes the control wall behaviour. Figure 5 represents the hysteresis loops of the control wall and the specimen strengthened with one layer of FRP. As can be seen from Figure 5, generally, the strength, the ductility and the dissipated energy of the control wall increased noticeably after strengthening.

Figure 6 shows the envelope curve of cyclic loading versus top deflection of the specimens. The SW character stands for strengthened wall and the following numbers represent number of FRP layers. Table 2 presents the details of the control wall and the strengthened walls SW1, SW2, SW3 and SW4. One can observe from the figure that the strength and the ductility of the specimens improved greatly by strengthening and increasing the number of FRP layers. However, adding the fourth layer caused less increase compared to other layers and further increase in FRP layers numbers seemed to approach no more change.

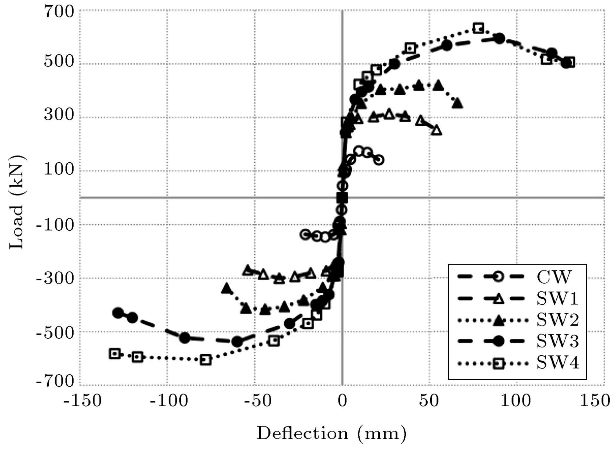

Figure 6. Envelope curve of hysteresis loops of specimens CW, SW1, SW2, SW3 and SW4.

In order to further study the seismic performance of the specimens, their hysteretic response characteristics, such as strength, ductility, dissipated energy and stiffness degradation, is represented. Figure 7(a) and (b) show the increasing of strength and the increasing of ductility versus the number of FRP layers, respectively. Ductility was estimated via calculating displacement ductility factor. It can be seen that strength and ductility approximately increase linearly up to adding the forth layer. However, adding the forth

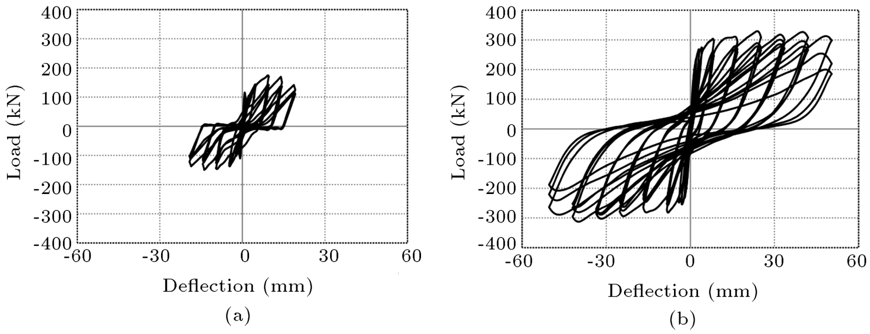

Figure 5. Comparison of hysteresis loops: (a) Control wall; and (b) strengthened wall with one layer of FRP.

Table 2. Details of the control wall and the strengthened walls SW1, SW2, SW3 and SW4.

Specimen	Section $b_w \times l_w$ (mm×mm)	Height h_w (mm)	Horiz. web reinf. (mm)	Vert. web reinf. (mm)	Vert. reinf. in boundary elements (mm)	Horiz. reinf. in boundary elements (mm)	Number of FRP layers
CW	100 × 1500	1795	Φ10@400	Φ10@280	Φ10@280	Φ10@80	0
SW1	100 × 1500	1795	Φ10@400	Φ10@280	Φ10@280	Φ10@80	1
SW2	100 × 1500	1795	Φ10@400	Φ10@280	Φ10@280	Φ10@80	2
SW3	100 × 1500	1795	Φ10@400	Φ10@280	Φ10@280	Φ10@80	3
SW4	100 × 1500	1795	Φ10@400	Φ10@280	Φ10@280	Φ10@80	4

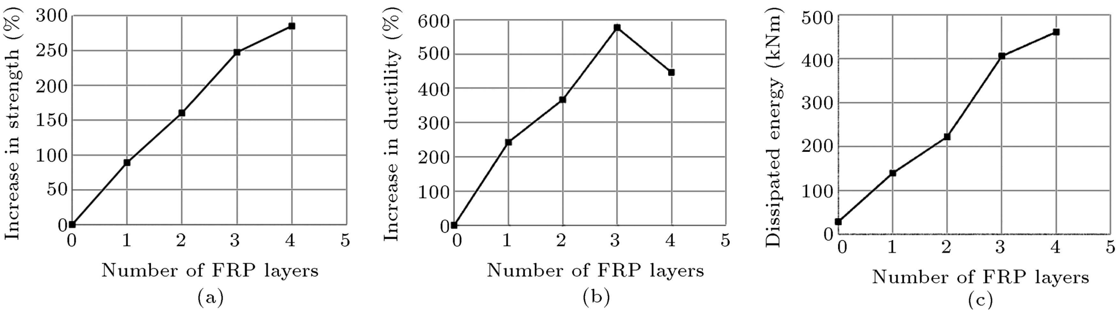

Figure 7. (a) Increase in strength versus number of FRP layers. (b) Increase in ductility versus number of FRP layers. (c) Dissipated energy versus number of FRP layers.

layer lead to less increase in strength and even decrease in ductility.

Shown in Figure 7(c) is the dissipated energy of specimens calculated by evaluating the area under the hysteresis loops up to the point that peak strength reduces by 20%. It can be seen from Figure 7(c) that the dissipated energy enhanced highly through strengthening, whereas adding the forth layer caused less increase compared to the other layers. The aforementioned behaviour which was also seen in strength and ductility of the specimens is because of premature shear failure.

In order to monitoring stiffness degradation, the variation of normalized stiffness with top horizontal deflection is illustrated in Figure 8. The normalized stiffness was estimated as the ratio of secant stiffness (K_i) and initial secant stiffness (K_0). It is clear from Figure 8 that the stiffness of CW was significantly lower than the other specimens. Furthermore, it is observed that CW had considerably severe stiffness degradation compared to strengthened specimens. It can be concluded that strengthening has a positive effect on stiffness degradation in the post-yielding stage of shear wall deformation. However, increase in the number of FRP layers slightly improves the stiffness degradation approach.

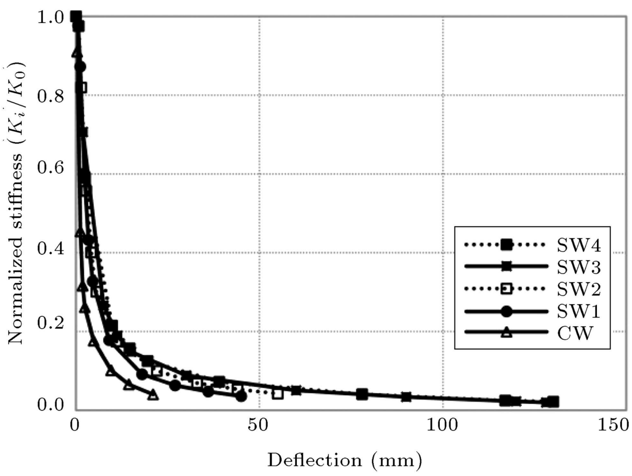

Figure 8. Normalized stiffness versus deflection.

5.2. Anchorage system

Flexural strengthening of the shear wall was provided by FRP laminates, with vertical fibers, bonded to the faces of the wall and anchored at the wall base with steel angels bolted to the support. In order to further study the effect of anchorage system on strengthening scheme, the failure modes of FRP peeling-off at anchorage zone and weak performance of anchorage system was ignored. Additionally, two specimens strengthened with three layers of FRP laminates were considered. Between these two specimens, only one of them strengthened using FRP laminates (SW3P), i.e. without applying anchorage system to serve as a reference for assessing the performance of the anchorage system.

Figure 9 shows the hysteresis loops obtained from numerical analysis of specimens SW3 and SW3P. It is clear from Figure 9 that due to presence of the anchorage system, the damage inflicted to strengthened shear wall SW3 was significantly delayed. Moreover, strength, ductility and dissipated energy of SW3 are substantially enhanced compared to SW3P based on the estimated value reported in Table 3. This enhancement in behaviour was due to the anchorage system shear strengthening besides its duty to anchor the FRP laminates. The anchorage system strengthened the base of the shear wall with steel angels in shear which delay the premature shear failure. In addition, it improved the hysteresis loops which increase the dissipated energy. It can be seen that this system of anchorage, i.e. steel angels bolted to support, considerably enhances the seismic performance of strengthened shear wall in flexure. It is worth pointing out that this improved performance depends on appropriate applying of anchorage system to avoid its weak working.

5.3. Horizontal web reinforcement ratio

As reported in [12], diagonal tension failure usually happens when shear wall has insufficient shear reinforcement. The diagonal tension failure has detrimental effect on ductile behaviour of shear wall. In order to show the effect of insufficient horizontal web reinforcement on the hysteresis loops, the percentage of

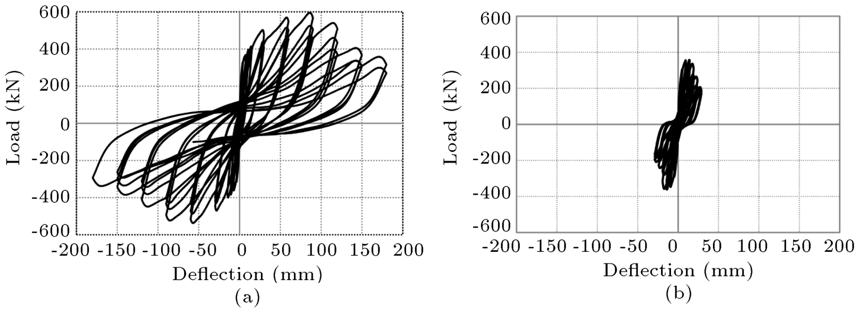

Figure 9. Hysteresis loops of specimens: (a) SW3; and (b) SW3P.

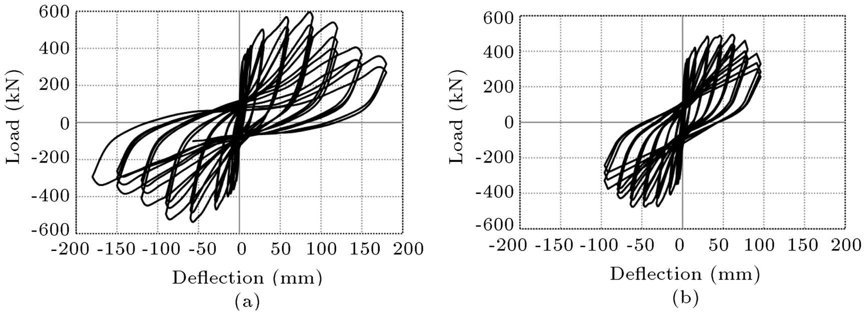

Figure 10. Comparison of hysteresis loops of strengthened wall with 3 layers of FRP with the horizontal web reinforcement ratio of (a) 0.39%, and (b) 0.25%.

Table 3. Hysteretic response characteristics of SW3 and SW3P.

Specimens	Strength (kN)	Displacement ductility factor	Dissipated energy
SW3P	360	9.2	45.2
SW3	559	35.6	406.5

horizontal web reinforcement in strengthened wall with three layer of FRP was reduced from 0.39% to 0.25%. Comparison of hysteresis loops shown in Figure 10 indicates that horizontal web reinforcement shortage can decrease desired wall behaviour such as strength and ductility.

Specifically, to study the influence of horizontal web reinforcement ratio on wall strengthening, its percentage in specimens was reduced from 0.39% to 0.25% and the number of FRP layers was increased from 1 to 3. Table 4 presents the list and details of selected specimens for numerical analysis of the strengthened shear wall with different number of FRP layers and various percentage of horizontal web reinforcement.

Figure 11 presents the envelope curves of the hysteresis loops obtained from numerical analysis of specimens SW1H1, SW1H2, SW2H1, SW2H2, SW3H1 and SW3H2. To further clarify the effect of the horizontal web reinforcement ratio, the envelope curves of specimens with the same number of FRP layers are shown in one diagram. As can be seen in Figure 11(a) and (b), the reduction of the horizontal reinforcement ratio has little influence on the envelope curves. However, as shown in Figure 11(c), reducing the horizontal reinforcement ratio leads to significant changes on the envelope curve of the wall strengthened by 3 FRP layers.

Table 4. Details of the strengthened wall with different horizontal web reinforcement ratio.

No.	Specimen	Section $b_w \times l_w$ (mm× mm)	Height h_w (mm)	ρ_h(%)	Horiz. web reinf. (mm)	Number of FRP layers
1	SW1H1	100 × 1500	1795	0.39	Φ10@400	1
2	SW1H2	100 × 1500	1795	0.25	Φ8@400	1
3	SW2H1	100 × 1500	1795	0.39	Φ10@400	2
4	SW2H2	100 × 1500	1795	0.25	Φ8@400	2
5	SW3H1	100 × 1500	1795	0.39	Φ10@400	3
6	SW3H2	100 × 1500	1795	0.25	Φ8@400	3

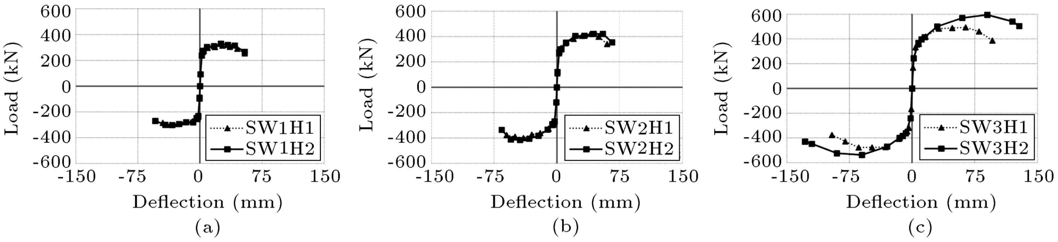

Figure 11. Envelope curves of the hysteresis loops of specimens SW1H1, SW1H2, SW2H1, SW2H2, SW3H1 and SW3H2.

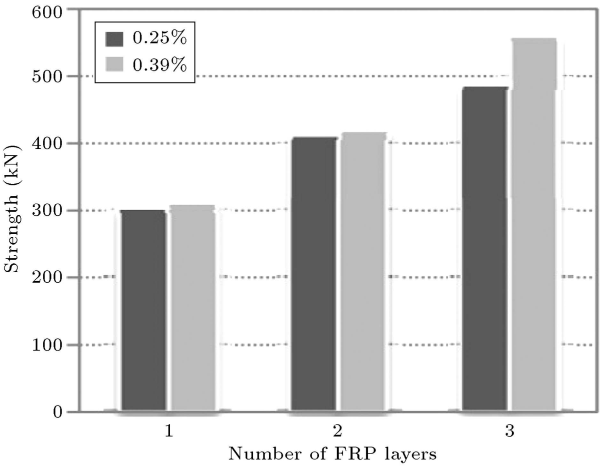

Figure 12. Strength comparison of specimens SW1H1, SW1H2, SW2H1, SW2H2, SW3H1 and SW3H2.

Figure 12 illustrates the strength of specimens versus the number of FRP layers in which the comparison of strength of specimens with the same number of FRP layers is shown close to each other. Based on the column chart, it appears that the reduction of the horizontal reinforcement ratio has little influence, i.e. less than 3%, on the strength of specimens SW1H1 and SW2H1. However, as can be seen, reducing the horizontal reinforcement ratio of specimen SW3H1 leads to significant changes on the strength, i.e. averagely 15.2%. The main reason is that the failure mode is changed to shear failure. In addition to the strength of the specimen SW3H2, its ductility reduced by averagely 33.3%.

In flexural strengthening, avoiding premature shear failure is essential. Thus, in spite of the anchorage system assist with the shear strengthening of wall, sufficient horizontal shear reinforcement is necessary. It is worth noting that with insufficient horizontal shear reinforcement, premature shear failure occurs and the increase in the vertical FRP laminates is useless.

5.4. Vertical web reinforcement ratio

Shear is more important compared to flexure in walls with small height to length ratio. Additionally, both horizontal and vertical shear reinforcements are necessary for shear wall. In addition to the dowel action, the vertical reinforcement provides a fastening force to the concrete in the urgent vicinity of the bars, and therefore helps to endure the sliding shear failure [22]. Figure 13 shows the effect of insufficient vertical web reinforcement on the hysteresis loops of strengthened wall with three layers of FRP. For this purpose, in Figure 13, a reduction in the percentage of vertical web reinforcement from 0.56% to 0.36% was considered. One can observe from Figure 13 that by decreasing vertical web reinforcement, the strength and the ductility is reduced.

Particularly, to study the influence of vertical web reinforcement ratio on wall strengthening, its percentage in specimens was reduced from 0.56% to 0.36% and the number of FRP layers was increased from 1 to 3, as considered in Section 5.3. Table 5 presents the list and details of selected specimens for numerical analysis of the strengthened shear wall with different number of FRP layers and various percentage of vertical web reinforcement.

The envelope curves of the hysteresis loops ob-

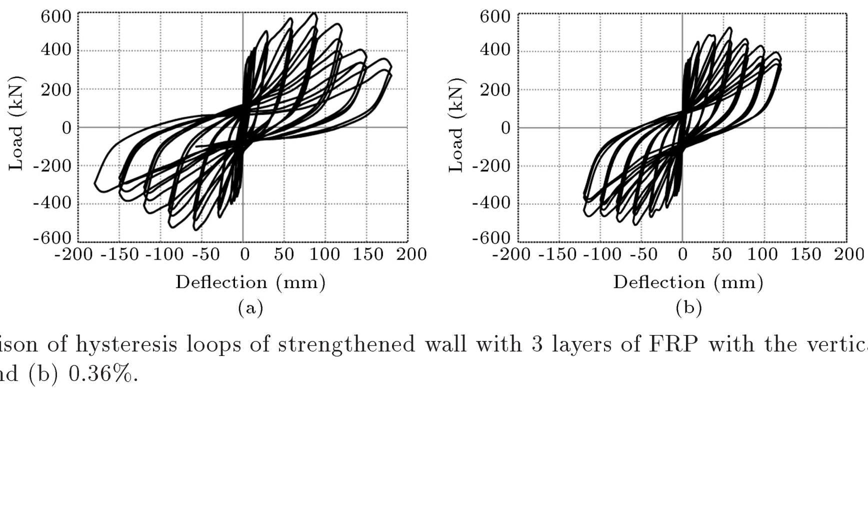

Figure 13. Comparison of hysteresis loops of strengthened wall with 3 layers of FRP with the vertical web reinforcement ratio of (a) 0.56%, and (b) 0.36%.

Table 5. Details of the strengthened wall with different vertical web reinforcement ratio.

No.	Specimen	Section $b_w \times l_w$ (mm× mm)	Height h_w (mm)	ρ_v(%)	Vert. web reinf. (mm)	Number of FRP layers
1	SW1V1	100 × 1500	1795	0.56	Φ10@280	1
2	SW1V2	100 × 1500	1795	0.36	Φ8@280	1
3	SW2V1	100 × 1500	1795	0.56	Φ10@280	2
4	SW2V2	100 × 1500	1795	0.36	Φ8@280	2
5	SW3V1	100 × 1500	1795	0.56	Φ10@280	3
6	SW3V2	100 × 1500	1795	0.36	Φ8@280	3

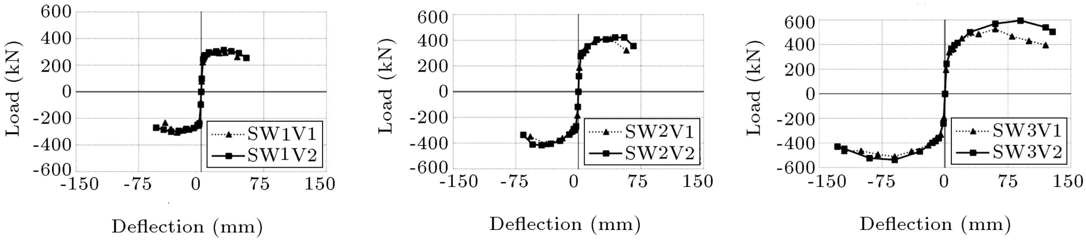

Figure 14. Envelope curves of the hysteresis loops of specimens SW1V1, SW1V2, SW2V1, SW2V2, SW3V1 and SW3V2.

tained from numerical analysis of specimens SW1V1, SW1V2, SW2V1, SW2V2, SW3V1 and SW3V2 are shown in Figure 14. To further clarify the effect of the vertical web reinforcement ratio, the envelope curves of the specimens with the same number of FRP layers are shown in one diagram. One can observe from Figure 14(a) and (b) that the reduction of the vertical reinforcement ratio has little influence on the envelope curves. However, as shown in Figure 14(c), reducing the vertical reinforcement ratio leads to significant changes on the envelope curve of the wall strengthened by 3 FRP layers similar to the horizontal reinforcement ratio results. The main reason is that the failure mode changes from flexural failure to shear failure.

Figure 15 shows the strength of specimens SW1V1, SW1V2, SW2V1, SW2V2, SW3V1 and SW3V2 versus the number of FRP layers. In this column chart, strength of specimens with the same number of FRP layers is shown close to each other. Based on Figure 15, it is clear that the reduction of the vertical reinforcement ratio has little effect on the strengths of specimens SW1V1 and SW2V1, i.e. less than 2%. However, reducing the vertical reinforcement ratio of specimen SW3V1 leads to more changes of the strength, averagely 7.9%. The aforementioned behaviour indicates that insufficient vertical reinforcement cause premature shear failure too. Moreover, in addition to the strength of specimen SW3V2, its displacement ductility decreased by averagely 17% is mainly governed by shear.

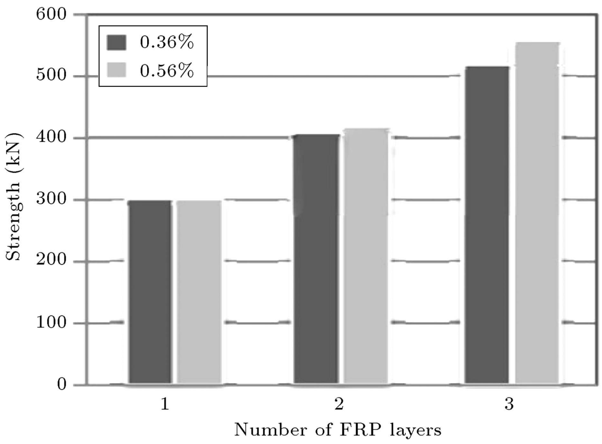

Figure 15. Strength comparison of specimens SW1V1, SW1V2, SW2V1, SW2V2, SW3V1 and SW3V2.

The results demonstrate that adequate horizontal and vertical shear rebar should be prepared to prevent premature shear failure in flexural strengthening. A temple of program prediction of wall cracked elements in premature shear failure mode and flexural failure mode is provided in Figure 16.

As can be seen from Figure 16, cracked elements for the case of shear failure mode are more focused in the web of wall with oblique direction. Whereas, in flexural failure mode, additional horizontal cracks can be seen in the boundary elements.

5.5. Vertical reinforcement ratio in boundary elements

The flexural capacity of the shear wall increases by concentrating the vertical reinforcement toward the boundary elements of the shear wall as long as the

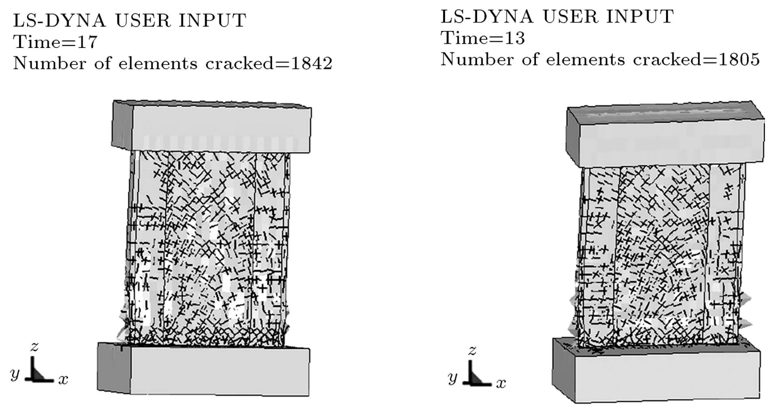

(a) (b)

Figure 16. Analytical model of failure modes: (a) Shear failure; and (b) flexural failure.

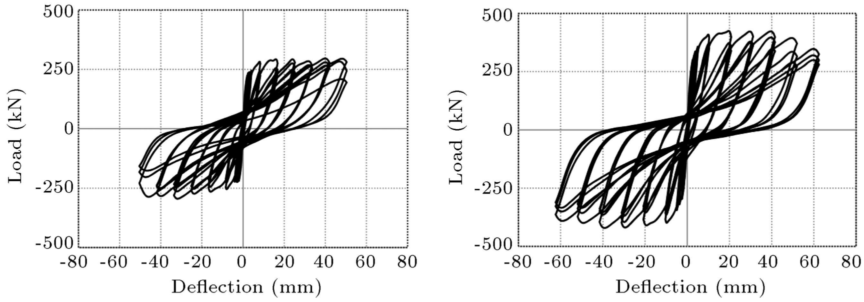

(a) (b)

Figure 17. Comparison of hysteresis loops: (a) SW1C1; and (b) SW1C3.

Table 6. Details of the strengthened wall with different vertical reinforcement ratio in boundary elements.

No.	Specimen	Section $b_w \times l_w$ (mm× mm)	Height h_w (mm)	ρ_c(%)	Vert. reinf. in boundary elements (mm)	Number of FRP layers
1	SW1C1	100 × 1500	1795	0.61	Φ10@280	1
2	SW1C2	100 × 1500	1795	0.95	Φ10@280	1
3	SW2C3	100 × 1500	1795	0.44	Φ10@280	1

shear failure mode can be prevented [23]. Present study was done by considering specimens with sufficient shear reinforcement and three different values of vertical reinforcements in boundary elements, which were SW1C1, SW1C2 and SW1C3. These specimens had one layer of FRP and identical reinforcement details, although their vertical reinforcement ratio in the walls boundary elements was not the same. Table 6 presents the details of the specimens SW1C1, SW1C2 and SW1C3.

For comparison, Figure 17 presents the hysteresis loops of specimens SW1C1 and SW1C3. As can be seen in this figure, the increase in vertical reinforcements in boundary elements enhances both the strength and the ductility.

Figure 18 shows the envelope curves of the hysteresis loops obtained from numerical analysis of specimens SW1C1, SW1C2 and SW1C3. In order to evaluate the effect of the vertical reinforcement ratio on

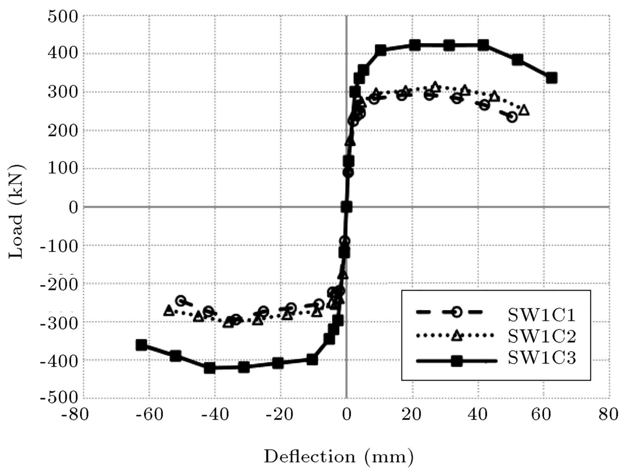

Figure 18. Envelope curves of hysteresis loops obtained from numerical analysis of specimens SW1C1, SW1C2 and SW1C3.

boundary elements, all the envelope curves are shown in one diagram.

As expected, increase in the vertical reinforcement ratio, in the boundary elements, leads to the strength enhancement. It is worth noting that due to sufficient shear capacity of the aforementioned specimens, the premature shear failure is prevented. Thus, the strength of the specimens, which is governed by flexure, is directly related to the vertical reinforcement ratio in the boundary elements. However, the ductility of specimens decreases by increasing in the amount of the boundary reinforcement. The ductility reduction is caused by decrease in the ultimate deflection and increase in the deflection at the yield point.

As a result, the increase in boundary reinforcement from 0.61% to 0.95% and from 0.95% to 2.4% increased the strength by 5% and 40%, respectively, and also decreased the ductility by 40% and 9%, respectively.

6. Conclusions

In this study, the numerical investigation, using LS-DYNA finite element program, to predict the behavior of RC squat shear wall strengthened in flexure by fiber reinforced polymer was performed. The accuracy of the presented model was acceptable in comparison with the experimental data. Then, the influence of number of FRP layers, presence of anchorage system and various reinforcement details on the behavior of the shear wall strengthened by the FRP laminates was studied. The following conclusions can be derived based on the numerical analysis of the studied shear walls:

1. Hysteretic response characteristics of the strengthened shear wall such as strength, ductility and dissipated energy were considerably affected by the increase of FRP layers. However, the rate of improvement was reduced beyond the addition of third layer.
2. The studied anchorage system, in addition to anchor FRP at the base of the shear wall, substantially enhanced the seismic performance of the strengthened wall by shear strengthening of its base.
3. The results showed that the behavior of the strengthened walls strongly depends on the amount of both horizontal and vertical web reinforcement ratio insufficient amount of which changes the failure mode to the shear failure. Thus, the proposed flexural strengthening scheme of this paper would be useless in this manner.
4. Both strength and ductility of the strengthened wall were considerably affected by the failure mode change to the shear failure.
5. Significant changes were observed in the behavior of the strengthened shear walls, when the amount of the vertical reinforcement in the boundary elements increased. Accordingly, increase in boundary reinforcement led to increase in strength, whereas the ductility decreased.
6. It can also be concluded that flexural capacity enhancement by increasing in the number of FRP layers and vertical reinforcement ratio in boundary elements is mainly dependent on the shear capacity of the strengthened shear walls.

Acknowledgment

Partial support of the Center of Excellence in Structure and Earthquake Engineering at Sharif University of Technology in conducting this research is greatly appreciated.

Nomenclature

f'_c	Cylinder compressive strength of concrete
f'_t	Uniaxial tensile strength of concrete
E_c	Initial tangent modulus of elasticity of concrete
v_c	Poisson's ratio of concrete
w	Crack width
σ_y	Yield stress of steel
v_s	Poisson's ratio of steel
E_s	Young's modulus of steel
S_1	Longitudinal tensile strength
S_2	Transverse tensile strength
S_{12}	Shear strength
C_2	Transverse compressive strength
α	Nonlinear shear stress parameter
$\bar{\tau}$	Fiber matrix shearing term
τ_{12}	Shear stress in (1-2) coordinate system
E_1	Young's modulus in direction 1
E_2	Young's modulus in direction 2
G_{12}	Shear modulus in (1-2) coordinate system
v_1	Poisson's ratio in direction 1
v_2	Poisson's ratio in direction 2
σ_2	Normal stress in direction 2
F_{matrix}	Matrix cracking failure criteria
F_{comp}	Compression failure criteria
F_{fiber}	Fiber breakage criteria

References

1. Meier, U., Deuring, M., Meier, H. and Schweger, G. "Strengthening of structures with CFRP laminates:

Research and application in Switzerland", *Proceeding of the1st Int. Conf. on Adv. Compos. Mater. in Bridges and Struct.*, Sherbrook, pp. 243-251 (1992).

2. Ritchie, P., Thomas, D., Lu, L-W. and Connelly, G. "External reinforcement of concrete beams using fiber reinforced plastics", *ACI Struct. J.*, **88**(4), pp. 490-500 (1991).

3. Saadatmanesh, H. and Ehsani, M. "RC beams strengthened with FRP plates II: Analysis and parametric study", *J. Struct. Eng. (ASCE)*, **117**(11), pp. 3434-3455 (1991).

4. Shahawy, M., Arockiasamy, M., Beitelman, T. and Sowrirajan, R. "Reinforced concrete rectangular beams strengthened with CFRP laminates", *Compos. Part B: Eng.*, **27**(3-4), pp. 225-233 (1996).

5. Priestley, M.J.N., Seible, F. and Fyffe, E. "Column seismic retrofit using fibreglass/epoxy jackets", *Proceeding of the 1st Int. Conf. on Adv. Compos. Mater. in Bridges and Struct.*, Sherbrooke, pp. 287-298 (1992).

6. Seible, F., Priestley, M.J.N., Hegemier, G.A. and Innamorato, D. "Seismic retrofit of RC columns with continuous carbon fiber jackets", *J. Compos. Construct. (ASCE)*, **1**(2), pp. 52-62 (1997).

7. Lombard, J., Lau, D.T., Humar, J.L., Foo, S. and Cheung, M.S. "Seismic strengthening and repair of reinforced concrete shear walls", *Proceeding of the 12th World Conf. on Earthq. Eng.*, New Zealand Society for Earthq. Eng., Silver stream, New Zealand, p. No. 2032 (2000).

8. Paterson, J. and Mitchell, D. "Seismic retrofit of shear walls with headed bars and carbon fibre wrap", *J. Struct. Eng. (ASCE)*, **129**(5), pp. 606-614 (2003).

9. Antoniades, K., Salonikios, T. and Kapppos, A. "Cyclic tests on seismically damaged reinforced concrete walls strengthened using fibre-reinforced polymer reinforcement", *ACI Struct. J.*, **100**(4), pp. 510-518 (2003).

10. Ghobarah, A. and Khalil, A.A. "Seismic rehabilitation of reinforced concrete walls using fibre composites", *Proceedings of the 13th World Conf. on Earthq. Eng.*, Vancouver, B.C, Canada, No. 3316 (2004).

11. Hallquist, J.O., *LS-DYNA Keyword User's Manual*, Livermore, CA: Livermore Softw. Tech. Co. (2009).

12. Paulay, T. and Priestly, M.J.N., *Seismic Design of Reinforced Concrete and Masonry Buildings*, John Wiley and Sons Inc., New York (1992).

13. Bao, X. and Li, B. "Residual strength of blast damaged reinforced concrete columns", *Int. J. Imp. Eng.*, **37**, pp. 295-308 (2010).

14. Arduini, M., Di Tommaso, A. and Nanni, A. "Brittle failure in FRP plate and sheet bonded beams", *ACI Struct. J.*, **94**(4), pp. 363-370 (1997).

15. Hu, H-T., Lin, F-M. and Jan, Y-Y. "Nonlinear finite element analysis of reinforced concrete beams strengthened by fiber-reinforced plastics", *Compos. Struct.*, **63**, pp. 271-281 (2004).

16. Ottosen, N.S. "A failure criterion for concrete", *J. Eng. Mech. Div. (ASCE)*, **103**(4), pp. 527-535 (1977).

17. Broadhouse, B.J. and Neilson, A.J. "Modeling reinforced concrete structures in DYNA3D", *Safety and Eng. Div., U.K. Atomic Energy Authority*, Winfrith, AEEW-M 2465 (1987).

18. Broadhouse, B.J. "The Winfrith concrete model in LS-DYNA3D", Report SPD/D(95)363: Struct. Performance Department, AEA Tech., Winfrith Tech. Center, U.K. (1995).

19. ACI Committee 318. *Building Code Requirements for Structural Concrete and Commentary (ACI 318M-08)*, American Concrete Institute, Detroit, MI (2008).

20. Chang, F.K. and Chang, K.Y. "A progressive damage model for laminated composites containing stress concentration", *J. Compos. Mater.*, **21**, pp. 834-855 (1987a).

21. Chang, F.K. and Chang, K.Y. "Post-failure analysis of bolted composite joint in tension or shear-out mode failure", *J. Compos. Mater.*, **21**, pp. 809-823 (1987b).

22. Paulay, T. "Design aspects of shear walls for seismic areas", *Can. J. Civ. Eng.*, **2**, pp. 321-344 (1975).

23. Paulay, T. "Earthquake-resisting shear wall - New Zealand design trends", *ACI Struct. J.*, **77**(3), pp. 144-152 (1980).

Biographies

Fariba Shadan received her BS degree in Civil Engineering, in 2007, from Isfahan University of Technology, Iran, and her MS degree in Structural Engineering, in 2011, from Sharif University of Technology, Tehran, Iran. She is currently pursuing her PhD degree at Amirkabir University of Technology, Tehran, Iran. Her research interests include finite element analysis, structural strengthening, structural dynamics, model updating and structural health monitoring.

Alireza Khaloo is Professor in the Faculty of Civil Engineering at Sharif University of Technology, Tehran, Iran. He received his BS degree in Civil Engineering, in 1979, from Texas University, Arlington (US), his MS degree in Structural Engineering, in 1981, from West Virginia State University (US), and his PhD degree in Structural Engineering, in 1986, from North Carolina State University (US). His research interests include topics related to structural engineering, reinforced concrete structures, concrete composite materials, materials of construction and earthquake engineering, such as constitutive relationships, modeling and testing structures and structural components and materials, shear capacity of HSC beams, fiber reinforced composite materials, high-strength normal and lightweight concrete, high performance concrete, durability of concrete in hot and aggressive environments, special concretes, RCC.

Parisa Shadan received her BS degree in Civil Engineering, in 2007, from Khaje Nasir Toosi University of Technology, Tehran, Iran and her MS degree in Structural Engineering, in 2011, from Amirkabir University of Technology, Tehran, Iran. She is currently pursuing her PhD degree at Amirkabir University of Technology, Tehran, Iran. Her research interests include structural strengthening, seismic behavior of structures, fracture mechanics, composite materials, finite element analysis and cohesive zone modeling.